Polymer Journal (2010) 42, 489–493

www.nature.com/pj

ORIGINAL ARTICLE

Development of acyl-bonded aminopropyl silica gel fillers with low interfacial adhesion energy in a polystyrene matrix

Yoshiya Senda[1], Jin Matsumoto[2], Takahiro Hidaka[2], Tsutomu Shiragami[2] and Masahide Yasuda[2]

To develop fillers that adhere closely to a matrix polymer and reduce the glass transition temperature (T_g) of filler/polymer composites, *N*-acyl-3-aminopropyl silica gel fillers (1) were prepared by the reaction of 3-aminopropyl silica gel (SiO_2–NH_2) and succinimidyl alkanoate (2) by controlling the amount and length of alkyl chains. The surface tension (γ) of 1 was measured by the wicking method. The interfacial adhesion energy (*W*) of composites (1/PS) between 1 and polystyrene (PS) was calculated using the dispersive component (γ^D) and the polar component (γ^P) of γ, according to the Equation ($W = 2\sqrt{\gamma_f^D \cdot \gamma_m^D} + 2\sqrt{\gamma_f^P \cdot \gamma_m^P}$) where subscripts *m* and *f* indicate matrix and filler, respectively. The *W* values of 1/PS composites were considerably smaller than those of the SiO_2–NH_2/PS composite. A good correlation between *W* and T_g showed that the introduction of acyl groups on SiO_2 was effective for the enhancement of adhesion between 1 and the matrix polymer. Moreover, it was confirmed that the addition of less than 30 wt% of 1 to PS did not affect the tensile strength of composites.
Polymer Journal (2010) **42,** 489–493; doi:10.1038/pj.2010.30; published online 21 April 2010

Keywords: adhesion energy; aminopropyl silica gel; glass transition temperature; interface energy; surface tension; tensile strength

INTRODUCTION

Modification of polymers with fillers is widely used to enhance the performance of polymers.[1,2] Inorganic materials such as talc,[3] calcium carbonate,[4,5] glass,[6,7] silica,[8,9] alumina,[10] zeolite[11–13] and wollastonite[14] have been widely used as fillers to improve mechanical performance such as the tensile strength and elongation strength of polymers. To enhance adhesion between inorganic fillers and the polymer matrix, organic additives such as maleic anhydride, carboxylic acids and silane-coupling reagents are mixed with the polymer.[4] However, problems such as the dispersibility of organic additives in the polymer, the increase in glass transition temperatures (T_g) and the elution of organic additives remain in the manufacturing process.

Recently, alkyl group-bonded zeolite[12] and wollastonite[14] fillers have been prepared to prevent the elution of organic additives from the polymer and to improve the handling of organic additives in the manufacturing process.[15] Silica gel filler is a stable and safe material that has a wide surface area and the ability to adsorb various materials. 3-Aminopropyl silica gel (SiO_2–NH_2)[16,17] can immobilize functional groups through a covalent bond. To develop a high-performance filler that achieves higher adhesion and a lower T_g of filler/polymer composites, the surface tension of the acyl-bonded SiO_2–NH_2 filler (**1**) can be modified by controlling the amount and length of alkyl chains (Scheme 1).

EXPERIMENTAL PROCEDURE

Instruments

^{1}H-nuclear magnetic resonance (NMR) (400 MHz) and ^{13}C-NMR (100 MHz) spectra were taken on a Bruker AV 400 M spectrometer (Bruker, Silberstrifen, Germany) for $CDCl_3$ solutions using SiMe4 as an internal standard. High-resolution mass spectra were taken on a Hitachi M2000A (Hitachi, Bremen, Germany) and a Bruker Daltonics Autoflex III TOF/TOF (Bruker) equipped with a matrix-assisted laser desorption/ionization apparatus. Fourier transform infrared was measured on a JASCO Herscel FT/IR-300 (JASCO, Hachioji, Japan) with a Micro-20 spectrometer. Scanning electron microscope images were recorded on a Hitachi S-4100.

Preparation of succinimidyl alkanoate (2)

A volume of 20 ml of CH_2Cl_2 solution containing alkanoic acid (0.5 mmol), *N*-hydroxy-succinimide (0.07 g, 0.6 mmol), *N*,*N*′-dicyclohexylcarbodiimide (0.12 g, 0.6 mmol) and 4-(dimethylamino)pyridine (0.06 g, 0.5 mmol) was stirred for 2 d at ambient temperature (Scheme 1). The reaction was monitored by TLC. The urea derived from *N*,*N*′-dicyclohexylcarbodiimide was removed by filtration and the solution was concentrated. The crude product was purified by silica gel column chromatography using $CHCl_3$–toluene–ethyl acetate (5:3:1) as the eluent and by repeated recrystallization from EtOH, resulting in **2** as a white solid.

Succinimidyl ethanoate (2a)

Yield 30.5%. Mp 131–133 °C. ^{1}H-NMR δ=2.35 (s, 3H), 2.84 (s, 4H), ^{13}C-NMR δ=17.5, 25.6, 165.6, 169.1; HRMS found: 157.0358. HRMS Calcd. for $C_6H_7NO_4$: 157.0375 [M^+].

[1]Asahi Organic Chemicals Co. Ltd, Nakanose, Nobeoka, Miyazaki, Japan and [2]Faculty of Engineering, Department of Applied Chemistry, University of Miyazaki, Gakuen-Kibanadai, Miyazaki, Japan
Correspondence: Professor M Yasuda, Faculty of Engineering, Department of Applied Chemistry, University of Miyazaki, 1-1,Gakuen Kibana-dai Nishi, Miyazaki 889-2192, Japan.
E-mail: yasuda@cc.miyazaki-u.ac.jp
Received 22 October 2009; revised 20 January 2010; accepted 17 March 2010; published online 21 April 2010

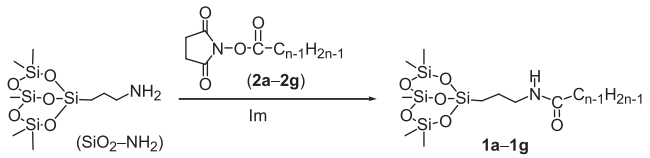

a; n= 2, b; n= 6, **c**; n= 10, **d**; n= 12, **e**; n= 14, **f**; n= 16, **g**; n= 18

Scheme 1 *N*-Acyl-3-aminopropyl silica gel fillers (**1a**–**g**).

Succinimidyl hexanoate (2b)

Yield 96.0%. Mp 34–37 °C. ^{1}H-NMR δ =0.91 (t, J=7.1 Hz, 3H), 1.34–1.41 (m, 4H), 1.71–1.79 (m, 2H), 2.60 (t, J=7.5 Hz, 2H), 2.83 (s, 4H); ^{13}C-NMR δ=13.7, 22.1, 24.2, 25.4, 25.6, 30.8, 168.7, 169.2; HRMS found: 213.1015. Calcd. for $C_{10}H_{15}NO_4$: 213.1001 [M^+].

Succinimidyl decanoate (2c)

Yield 70.5%. Mp 54–56 °C. ^{1}H-NMR δ=0.88 (t, J=6.8 Hz, 3H), 1.33–1.41 (m, 12H), 1.74 (quint, J=7.6 Hz, 2H), 2.60 (t, J=7.6 Hz, 2H), 2.83 (s, 4H); ^{13}C-NMR δ=14.1, 22.6, 24.6, 25.6, 28.8, 29.1, 29.2, 29.3, 30.9, 31.8, 168.7, 169.1; HRMS found: 269.1656. Calcd. for $C_{14}H_{23}NO_4$: 269.1627 [M^+].

Succinimidyl dodecanoate (2d)

Yield 82.4%. Mp 61–63 °C. ^{1}H-NMR; δ=0.88 (t, J=6.8 Hz, 3H), 1.26–1.42 (m, 16H), 1.70–1.78 (quint, J=8.0 Hz, 2H), 2.60 (t, J=7.2 Hz, 2H), 2.83 (s, 4H); ^{13}C-NMR δ=14.1, 22.7, 24.6, 25.6, 28.8, 29.1, 29.3, 29.3, 29.5, 29.5, 30.9, 31.9, 168.7, 169.1. MALDI-MS found: 320.1835. Calcd. for $C_{16}H_{27}NO_4Na$: 297.1838 [M+Na$^+$].

Succinimidyl tetraadecanoate (2e)

Yield 74.7%. Mp 81–83 °C. ^{1}H-NMR δ=0.88 (t, J=7.08 Hz, 3H), 1.26–1.42 (m, 20H), 1.70–1.78 (quint, J=7.4 Hz, 2H), 2.60 (t, J=7.44 Hz, 2H), 2.83 (s, 4H). ^{13}C-NMR δ=14.1, 22.7, 24.6, 25.6, 25.6, 28.8, 29.1, 29.3, 29.5, 29.6, 29.6, 29.6, 30.9, 31.9, 168.7, 169.2. HRMS found: 325.2176. Calcd. for $C_{18}H_{31}NO_4$: 325.2253 [M^+].

Succinimidyl hexadecanoate (2f)

Yield 62.0%. Mp 82–84 °C. ^{1}H-NMR δ=0.88 (t, J=6.8 Hz, 3H), 1.26–1.42 (m, 24H), 1.70–1.78 (quint, J=7.6 Hz, 24H), 2.60 (t, J=7.2 Hz, 2H), 2,83 (s, 4H); ^{13}C-NMR δ=14.1, 22.7, 24.6, 25.6, 25.6, 28.8, 29.1, 29.3, 29.5, 29.6, 29.6, 29.7, 30.9, 31.9, 168.7, 169.1. MALDI-MS found: 376.2446. Calcd. for $C_{20}H_{35}NO_4$-Na: 376.2464 [M+Na$^+$].

Succinimidyl octadecanoate (2g)

Yield 88.0%. Mp 91–92 °C. ^{1}H-NMR δ =0.88 (t, J=6.9 Hz, 3H), 1.26–1.42 (m, 28H), 1.74 (quint, J=7.51 Hz, 2H), 2.60 (t, J=7.5 Hz, 2H), 2.83 (s, 4H); ^{13}C NMR δ 14.1, 22.7, 24.6, 25.6, 28.8, 29.1, 29.3, 29.5, 29.6, 29.6, 29.6, 29.6, 29.6, 29.6, 29.7, 30.9, 31.9, 168.7, 169.2; HRMS found: 381.2866. Calcd. for $C_{22}H_{39}NO_4$: 381.2879 [M^+].

Quantitative analysis of 1 by infrared absorption spectrophotometry

For calibration lines, RCO_2H was mixed with SiO_2–NH_2 in a given ratio of M_R to W_S, where M_R and W_S denote the molar amounts of RCO_2H and the weight of SiO_2–NH_2, respectively. *N*-Benzylacetamide and *N*-phenylhexanamide were used instead of oily acetic acid and hexanoic acid. The M_R/W_S were plotted against the area ratio (A_R/A_S) of the C–H stretching of the RCO– group at 3000–2830 cm^{-1} to the Si–O stretching of SiO_2–NH_2 at 800 cm^{-1}, which were obtained from the absorbance mode in the infrared (IR) spectra of the mixed samples. Compound **1** was ground on a mortar and subjected to IR absorption spectrophotometry. Quantitative analysis was performed using the A_R/A_S of **1** and the calibration line.

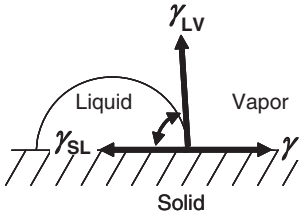

Figure 1 Contact angles (θ) and surface tensions among vapor, liquid and solid surfaces.

Measurement of contact angle

The surface tension (γ) of the solid is related to surface tensions in solid–liquid (γ_{SL}) and liquid–vapor (γ_{LV}) using the contact angle (θ), as shown in Figure 1. The surface tension γ of PS was determined from θ, which was measured at 23 °C by the sessile drop method[14] using test liquids such as CH_2I_2, H_2O and formamide. The average θ values of five drops were taken 10 s after drop deposition.

The γ of **1** was measured by the wicking method reported by Kim and co-workers.[12] Glass capillaries with a 100 mm length and 1.0 mm diameter were plugged at the bottom with a small wad of cotton wool. Well-dried **1** (40 mg) was filled into the capillary up to a height of 70 mm. The penetration distance (h in cm) of the probe liquids through the column packed with **1** was measured at 23 °C in a given time (t in seconds). Parameter h can be related to t and θ by Washburn's Equation, Equation (1),[18,19,20] using the effective interstitial pore radius (R in cm), viscosity (η in cP) and the interfacial tension of liquid–vapor (γ_{LV}) of the probe liquid (*Electronic Supporting Information available*: The following data are included: the properties of probe liquids such as hexane, heptane, octane, water, CH_2I_2 and formamide, the plots of h^2 versus time **1a** as typical example, the plots of $2\eta h^2/t$ versus γ_{LV} for wicking with alkanes in the measurement of the surface tensions, and differential scanning calorimetry (DSC) profiles of **1**/PS. See Supplementary Information).

When hexane, heptane and octane, which has a θ value of nearly zero, were used as spreading liquids, Equation (1) could be changed to Equation (2).[12] According to Equation (2), R was determined by the plot of h^2/t against the $\gamma_{LV}/(2\eta)$ of solvents. The R-values obtained for **1** are listed in Table 1. Using CH_2I_2, H_2O and formamide as the probe liquids with $\theta > 0$, the plots of h^2 against t produced a straight line with the slope of $R\gamma_{LV}\cos\theta/(2\eta)$, which was plotted against $R\gamma_{LV}/(2\eta)$ to yield θ-values of **1** toward each of the solvents (Table 1).

$$h^2 = \frac{R\gamma_{LV}\cos\theta}{2\eta}t \quad (1)$$

$$\frac{h^2}{t} = R\frac{\gamma_{LV}}{2\eta} \quad (2)$$

Calculation of surface tension components

According to Equation (3),[12] the dispersive Lifshitz–van der Waals component (γ^D) of **1** was determined using the $\cos\theta$ value when CH_2I_2 ($\gamma^-_{LV}=\gamma^+_{LV}=0$, $\gamma_{LV}=\gamma^D_{LV}=50.8$ mJ m^{-2}) was used as the penetration probe solvent. In addition, the Lewis acid (γ^+) and Lewis base (γ^-) components were determined using the $\cos\theta$ values obtained from the measurements in H_2O and formamide, the surface tension components of which are shown in the supporting information (*Electronic Supporting Information available*: The following data are included: the properties of probe liquids such as hexane, heptane, octane, water, CH_2I_2 and formamide, the plots of h^2 versus time **1a** as typical example, the plots of $2\eta h^2/t$ versus γ_{LV} for wicking with alkanes in the measurement of the surface tensions, and DSC profiles of **1**/PS. See Supplementary Information). The polar component (γ^P) due to the Lewis acid–base contribution was calculated by Equation (4) using γ^+ and γ^-. The γ of **1** was obtained by the summation of γ^D and γ^P (Equation (5)).

Table 1 Effective interstitial pore radius (*R*), contact angle (θ), surface tension (γ), interfacial adhesion energy (*W*) and glass tension temperature (T_g) for acyl-bonded silica-gel microbeads

Samples[a]	Yield[b] (%)	R[c] (10^{-5}cm)	θ (°)[d] H_2O	CH_2I_2	FA	γ^D (mJ m^{-2})	γ^+ (mJ m^{-2})	γ^- (mJ m^{-2})	γ^P (mJ m^{-2})	γ (mJ m^{-2})	W[e] (mJ m^{-2})	T_g[f] (°C)
SiO_2–NH_2	—	2.6	39.0	39.5	29.6	39.9	0.9	37.1	11.5	51.3	79.1	97.6
1a (0.47)	(31)	3.2	61.5	41.6	50.4	38.8	0.3	21.4	4.7	43.5	71.6	94.3
1b (0.07)	(5)	3.0	60.9	46.3	54.5	36.3	0.1	25.5	3.1	39.4	68.6	92.4
1b (0.19)	(13)	3.0	76.3	51.6	63.1	33.4	0.1	11.8	2.5	35.9	65.5	91.6
1b (0.52)	(34)	3.1	74.4	56.6	62.5	30.6	0.4	13.4	4.5	35.0	63.9	91.1
1b (0.75)	(50)	3.5	86.5	68.2	73.3	23.9	0.4	7.3	3.5	27.4	56.5	77.9
1b (0.85)	(56)	4.3	90.0	76.5	81.9	19.3	0.2	8.8	2.6	21.9	50.6	76.9
1c (0.08)	(5)	2.6	63.0	24.3	19.7	46.4	1.6	6.9	6.5	53.0	78.7	92.8
1c (0.20)	(11)	3.4	75.2	58.8	53.1	29.3	1.4	7.3	6.3	35.6	63.4	92.5
1c (0.44)	(29)	3.5	83.4	59.7	68.2	28.7	0.3	7.5	3.2	31.9	61.5	92.0
1c (0.68)	(45)	2.9	90.0	70.9	79.5	22.4	0.1	7.5	1.7	24.1	53.7	89.3
1c (0.86)	(57)	3.7	90.0	78.1	84.5	18.5	0.0	10.4	0.6	19.1	48.0	82.4
1d (0.88)	(59)	4.3	90.0	87.5	89.9	13.8	0.0	14.1	1.2	15.0	42.3	84.3
1e (0.87)	(58)	3.0	90.0	81.1	86.2	16.9	0.0	11.5	0.9	17.8	46.3	86.9
1f (0.81)	(54)	3.4	90.0	88.7	89.8	13.3	0.1	13.9	2.5	15.8	42.5	91.6
1 g (0.10)	(7)	2.3	56.8	37.7	49.0	40.7	0.1	27.0	2.4	43.1	72.0	93.1
1 g (0.17)	(11)	3.0	79.1	54.3	64.5	31.9	0.2	9.7	3.1	34.9	64.4	92.2
1 g (0.47)	(31)	2.4	90.0	69.0	79.2	23.4	0.0	7.4	0.8	24.2	54.0	85.2
1 g (0.66)	(44)	4.5	90.0	85.4	87.3	14.8	0.2	12.1	2.8	17.7	44.9	83.3
PS[g]		—	59.0	67.0	49.6	29.2	0.1	2.0	1.0	30.1	—	89.9

[a]The values in the parentheses are the amounts (x_R/mmol g^{-1}) of acyl groups in **1**. Measurement of surface tensions by wicking method at 20 °C.
[b]Yields based on $100x_R/x_A$.
[c]Effective interstitial pore radius.
[d]Contact angle.
[e]The adhesion force (*W*) calculated by Equation (6).
[f]Glass transition temperature was measured on differential scanning calorimetry at 10 °C min^{-1} for the **1**/PS (10%) preheated at 190 °C. T_g of polystyrene (PS) was 89.9 °C.
[g]Measured by the sessile drop method.

These results are shown in Table 1.

$$\gamma_{LV}(1+\cos\theta) = 2\left(\sqrt{\gamma^D \cdot \gamma^D_{LV}}+\sqrt{\gamma^+ \cdot \gamma^-_{LV}}+\sqrt{\gamma^- \cdot \gamma^+_{LV}}\right) \quad (3)$$

$$\gamma^P = 2\sqrt{\gamma^+ \cdot \gamma^-} \quad (4)$$

$$\gamma = \gamma^D+\gamma^P \quad (5)$$

Preparation of 1/PS composites

A polystyrene pellet (PS; ρ=1.04–1, 05 g cm^{-3}, Japan Polystyrene G590N) was dissolved in tetrahydrofuran. The given percents by weight % (1, 5, 10 and 30 wt%) of **1** were added to the tetrahydrofuran solution of the PS. The PS solution containing **1** was poured on a Teflon plate that was surrounded by a barrier and dried to yield the **1**/PS composite film. As a reference, SiO_2/PS and SiO_2–NH_2/PS composites were prepared in a similar manner. The prepared composites were subjected to scanning electron microscope observation, DSC measurement and tensile testing.

Measurement of the tensile strength (σ) of composites

The **1**/PS film was introduced into a handy injection molding machine (Shinko Sellbic, Japan), melted at a temperature of 260 °C, and injected into a dumbbell shape of 65×10×2 mm to fabricate the test piece of **1**/PS composites. Similarly, a test piece of a composite of PS with SiO_2 (SiO_2/PS) was prepared as a reference material. Tensile tests of composites were carried out using a universal testing machine at a crosshead speed of 10 mm min^{-1} at a temperature of 23 °C. Tensile strength (σ) was determined from stress-strain curves according to ASTM D638.

DSC Measurement of 1/PS composites.

A piece of **1**/PS film (5.0 mg) was packed in an aluminum pan and sealed to prepare samples for DSC. In general, the DSC profile was dependent on the preheated temperature. After the samples were preheated up to 190 °C and then cooled to room temperature, DSC charts were recorded at a temperature-increasing rate of 10 °C min^{-1} on a Rigaku Thermo plus DSC 8240 (Rigaku, Akishima, Japan). The T_g of **1**/PS and SiO_2–NH_2/PS is listed in Table 1 and thermograms are shown in the supporting information (*Electronic Supporting Information available*: The following data are included: the properties of probe liquids such as hexane, heptane, octane, water, CH_2I_2 and formamide, the plots of h^2 versus time **1a** as typical example, the plots of $2\eta h^2/t$ versus γ_{LV} for wicking with alkanes in the measurement of the surface tensions, and DSC profiles of **1**/PS. See Supplementary Information).

RESULTS AND DISCUSSION

Preparation of acyl-bonded SiO_2–NH_2 fillers (1)

N-Acyl-3-aminopropyl silica gels (**1a–g**) were prepared by a reaction of succinimidyl alkanoate (**2a–g**) with SiO_2–NH_2 (average diameter of beads: 8.3 μm; pore volume: 0.59 cm^3 g^{-1}; amount of NH_2 (x_A): 1.50 mmol g^{-1}, Fuji Silysia Chemical, Kasugai, Japan) in the presence of imidazole for 3 days. The characteristic absorptions of the IR spectra of **1** were assigned by a comparison with that of *N*-propyl-4-octadecanamide (**3**), which was a reference sample prepared by a reaction of **2 g** with n-PrNH_2 in the presence of imidazole (Figure 2). Absorption near 1560 cm^{-1} can be assigned to an N–H bending of the amide bond (a_1). A C–H bending of the methyl group (a_2) and a C–H stretching mode (a_3) appeared at 1470 and 3000–2850 cm^{-1}, respectively. The SiO_2–NH_2 exhibited strong Si–O absorption at 800 cm^{-1} (a_4), as well as at 1700–1660 and 1300–900 cm^{-1}.

The amount of acyl groups (x_R/mmol g^{-1}) that bonded to SiO_2–NH_2 in **1** was analyzed by IR absorption spectrophotometry at a_3 and a_4. Figure 3 shows plots of x_R versus a given amount of **2b, 2c** and **2 g** used in the preparation of **1**. As the amount of **2** increased, the x_R

of **1b**, **1c** and **1 g** increased gradually to reach a maximum point near 1.50 mmol g^{-1} of **2**, which was equal to x_A (=1.50 mmol g^{-1}). At the maximum point, the yields ($100x_R/x_A$) based on x_A were determined to be 56, 52 and 44% for **1b**, **1c** and **1 g**, respectively. Similarly, the maximum yields of **1a**, **1d**, **1e** and **1f** were 31, 59, 58 and 54 %, respectively.

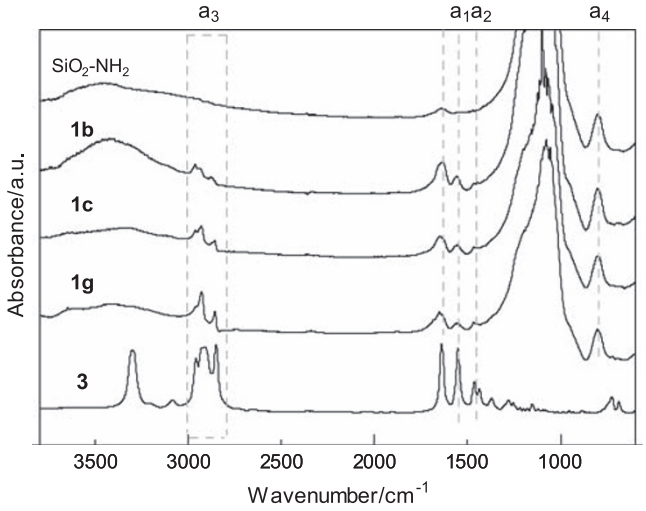

Figure 2 IR spectra of **1a–c** along with those of SiO_2–NH_2 and *N*-propyl-4-octadecanamide (**3**) in the region 600–3800 cm^{-1}. a_1: The N–H bending of the amide bond near 1560 cm^{-1}; a_2: the bending mode of C–H at 1470 cm^{-1}; a_3: the stretching mode of C–H at 3000–2830 cm^{-1}; and a_4: the Si–O stretching mode at 800 cm^{-1}.

Morphology and tensile strength (σ) of 1/PS composites

Scanning electron microscope images of the **1**/PS and SiO_2/PS composites were observed to examine the adhesion of **1** with the PS matrix (Figure 4). In the scanning electron microscope images of the cross-section of SiO_2/PS composites, a void appeared at the interface between SiO_2 particles and the PS matrix, showing that the adhesion of SiO_2 toward PS was poor. In the case of **1**/PS, on the other hand, **1** was well dispersed over the PS matrix, and the PS matrix adhered closely to **1** compared with SiO_2/PS. With an increase in the alkyl chain length from C_6 to C_{18}, the void decreased, resulting in the higher adhesion of **1** in PS.

The tensile strength (σ) of the SiO_2/PS composite decreased to 37.3 MPa from 46.0 MPa of PS when 30 wt% of SiO_2 was added to the PS (Figure 5). In the case of **1**/PS composites, on the other hand, the addition of 30 wt% of **1** maintained the σ-values of 44–45 MPa the same as the σ-value of PS. Thus, the introduction of acyl groups on SiO_2 was effective for the enhancement of adhesion between **1** and the matrix polymer.

Interfacial adhesion energy between the filler and matrix polymer

The interfacial adhesion energy (W) between the filler and the matrix polymer is one of the most important properties of composites.[14] Švab *et al.*[14] have postulated that γ^D and γ^P can be regarded in the solid state as the dispersive and polar components of the surface energy, respectively. Moreover, they proposed that W can be represented by Equation (6) using the surface free energy (surface tension)

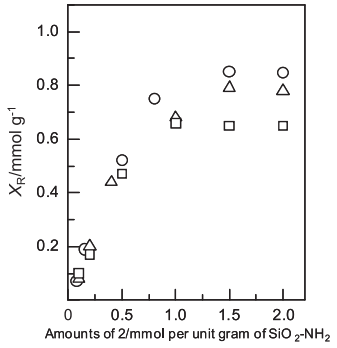

Figure 3 Plots of the amount of acyl groups (x_R) versus the amount of **2b** (○), **2c** (△) and **2 g** (□) used in the reaction of **2** with SiO_2–NH_2.

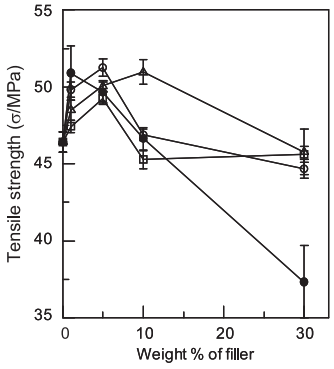

Figure 5 The additive effect of SiO_2 (●), **1a** (○), **1b** (△) and **1c** (□) on the tensile strength (σ) of PS.

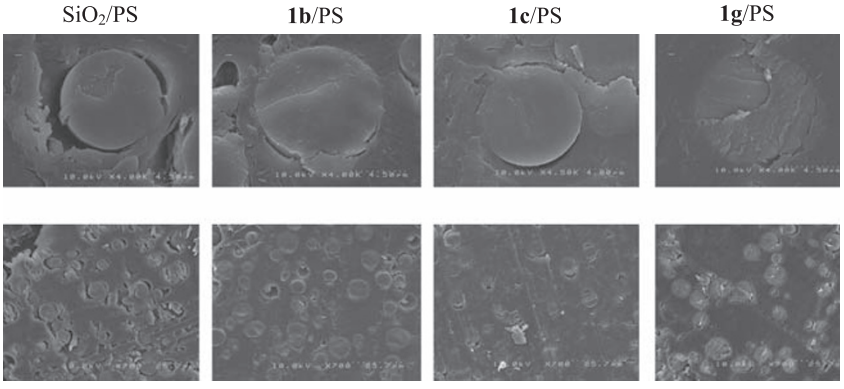

Figure 4 The scanning electron microscope images of the cross-sections of **1**/PS composites and SiO_2/PS composites under ×700 (lower) and ×4000 (upper) magnifications.

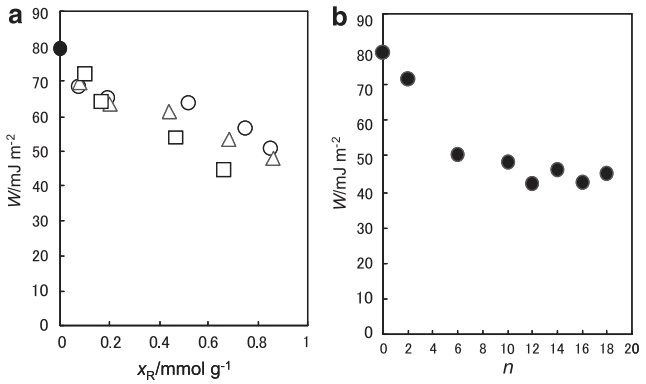

Figure 6 (**a**) Dependence of x_R on W in **1b** (○), **1c** (△) and **1 g** (□) along with SiO_2–NH_2 (●). (**b**) Dependence of carbon number (n) on W.

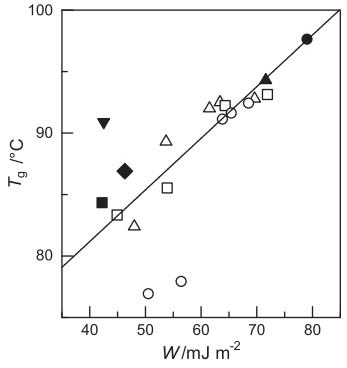

Figure 7 Relationship between T_g and W: SiO_2–NH_2/PS (●), **1a/**PS (▲), **1b**/PS (○), **1c/**PS (△), **1d/**PS (■), **1e/**PS (◆), **1f/**PS (▼) and **1g/**PS (□).

of the filler (γ_f) and matrix (γ_m) and the interfacial free energy (γ_{mf}) between the filler and matrix polymer. The γ_{mf} was obtained by Equation (7) using components γ^D and γ^P of the filler and matrix polymer.[14,21] Therefore, W-values can be calculated according to Equation (8), where subscripts m and f indicate matrix and filler, respectively.

$$W = \gamma_f + \gamma_m - \gamma_{mf} \quad (6)$$

$$\gamma_{mf} = \gamma_f + \gamma_m - 2\sqrt{\gamma_f^D \cdot \gamma_m^D} - 2\sqrt{\gamma_f^P \cdot \gamma_m^P} \quad (7)$$

$$W = 2\sqrt{\gamma_f^D \cdot \gamma_m^D} + 2\sqrt{\gamma_f^P \cdot \gamma_m^P} \quad (8)$$

The W values of the **1**/PS composites were calculated according to Equation (8) using the γ^D and γ^P of **1** and PS listed in Table 1. The dependence of W values on x_R was examined in the cases of **1b**, **1c** and **1 g** (Figure 6a). With an increase in x_R, W values decreased gradually. In addition, W values decreased as the carbon number (n) on the acyl group of **1** increased (Figure 6b). As shown in Table 1, the γ of **1** was strongly affected by the γ^D component, whereas the polar γ^P contributions were small because of the hydrophobic acyl chains on **1**. On the other hand, SiO_2–NH_2 had relatively large values of γ^P. These results showed that the interaction energy between **1** and the hydrophobic PS matrix was weaker, as the hydrophobic character of **1** increased because of increases in x_R and n.

Relationship between W and T_g

The T_g is one of the most important characteristics of polymer materials. T_g is used as a parameter to evaluate the adhesion of filler toward the matrix.[22,23] The T_g values of **1**/PS and SiO_2–NH_2/PS composites measured by DSC are shown in Table 1. The T_g of **1**/PS composite was lower than that of the SiO_2–NH_2/PS composite. Moreover, T_g decreased with an increase in x_R of **1b, 1c** and **1g**. Figure 7 shows the correlation between T_g and W, revealing that the introduction of acyl groups on SiO_2 was effective to enhance the adhesion between **1** and the matrix polymer.

In conclusion, intrafacial adhesion energy (W) can be modified by γ, which is easily controlled by the amount and length of hydrophobic alkyl chains. It was found that lower W values led to close adhesion and lower T_g.

1 Rothon, R. *Particulate-Filled Polymer Composites* (Longman Scientific and Technical: Harlow, 1995).
2 Móczó, J. & Pukánszky, B. Polymer micro and nanocomposites: structure, interactions, properties. *J. Ind. Eng. Chem.* **14,** 535–563 (2008).
3 Rotzinger, B. Talc-filled PP: a new concept to maintain long term heat stability. *Polym. Degrad. Stab.* **91,** 2884–2887 (2006).
4 Demjén, Z., Pukánszky, B. & Nagy, J. Evaluation of interfacial interaction in polypropylene/surface treated $CaCO_3$ composites. *Composites Part A* **29,** 323–329 (1998).
5 Zuiderduin, W. C. J., Westzaan, C., Huétink, J. & Gaymans, R. J. Toughening of polypropylene with calcium carbonate particles. *Polymer* **44,** 261–275 (2003).
6 Sánchez-Soto, M., Pagés, P., Lacorte, T., Briceño, K. & Carrasco, F. Curing FTIR study and mechanical characterization of glass bead filled trifunctional epoxy composites. *Compos. Sci. Technol.* **67,** 1974–1985 (2007).
7 DiBenedetto, A. T. Tailoring of interfaces in glass fiber reinforced polymer composites: a review. *Mater. Sci. Eng., A* **302,** 74–82 (2001).
8 Yatsuyanagi, F., Suzuki, N., Ito, M. & Kaidou, H. Effects of surface chemistry of silica particles on the mechanical properties of silica filled styrene-butadiene rubber systems. *Polym. J.* **34,** 332–339 (2002).
9 Elias, L., Fenouillot, F., Majeste, J. C. & Cassagnau, P. Morphology and rheology of immiscible polymer blends filled with silica nanoparticles. *Polymer* **48,** 6029–6040 (2007).
10 Tallman, D. E., Levine, K. L., Siripirom, C., Gelling, V. G., Bierwagen, G. P. & Croll, S. G. Nanocomposite of polypyrrole and alumina nanoparticles as a coating filler for the corrosion protection of aluminium alloy 2024-T3. *Appl. Surf. Sci.* **254,** 5452–5459 (2008).
11 Berry, M. B., Libby, B. E., Rose, K., Haas, K- H. & Thompson, R. W. Incorporation of zeolites into composite matrices. *Microporous Mesoporous Mater.* **39,** 205–217 (2000).
12 Lee, J. Y., Lee, S. H. & Kim, S. W. Surface tension of silane treated natural zeolite. *Mater. Chem. Phys.* **63,** 251–255 (2000).
13 Metin, D., Tihminlioğlu, F., Balköse, D. & Ülkü, S. The effect of interfacial interactions on the mechanical properties of polypropylene/natural zeolite composites. *Composites Part A* **35,** 23–32 (2004).
14 Švab, I., Musil, V. & Leskovac, M. The adhesion phenomena in polypropylene/wollastonite composites. *Acta Chim. Slov.* **52,** 264–271 (2005).
15 Yokoyama, R., Suzuki, S., Shirai, K., Yamauchi, T., Tsubokawa, N. & Tsuchimochi, M. Preparation and properties of biocompatible polymer-grafted silica nanoparticle. *Eur. Polym. J.* **42,** 3221–3229 (2006).
16 Senda, Y., Hidaka, T., Matsumoto, J., Shiragami, T. & Yasuda, M. Synthesis and characterization of *o*-hydroxybenzophenone chromophore bonded to aminopropyl silica gel-microbeads,. *Bull. Chem. Soc. Jpn.* **81,** 1518–1524 (2008).
17 Jal, P. K., Patel, S. & Mishra, B. K. Chemical modification of silica surface by immobilization of functional groups for extractive concentration of metal ions. *Talanta* **62,** 1005–1028 (2004).
18 Carino, L. Kinetics of wetting of a compacted powder by aqueous solutions of surface active agents. *Colloid Polym. Sci.* **254,** 108–113 (1976).
19 Siebold, A., Nardin, M., Schultz, J., Walliser, A. & Oppliger, M. Effect of dynamic contact angle on capillary rise phenomena. *Colloids Surf., A* **161,** 81–87 (2000).
20 Wu, S. *Polymer Interface and Adhesion 236–246* (Marcel Dekker: New York, 1982).
21 Good, R. J. *Contact Angle Wettability and Adhesion* 3th ed Mittal, K.L. (VSP, 1993).
22 Herrero, C. R., Morales, E. & Acosta, J. L. Compatibilization of semicrystalline polymeric alloys through sepiolite addition. *J. Appl. Polym. Sci.* **412,** 1189–1197 (1990).
23 Vrsaljko, D., Leskovac, M., Blagojević, S. L. & Kovačević, V. Interphase phenomena in nanoparticulate filled polyuretane/poly(vinyl acetate) polymer systems. *Polym. Eng. Sci.* **48,** 1931–1938 (2008).

Supplementary Information accompanies the paper on Polymer Journal website (http://www.nature.com/pj)